Arab J Sci Eng (2016) 41:4509–4516
DOI 10.1007/s13369-016-2177-4

RESEARCH ARTICLE - MECHANICAL ENGINEERING

Experimental Study on Thermal Performance of a Novel Solar Air Collector Having Conical Springs on Absorber Plate

Mesut Abuşka[1] · **Mehmet Bahattin Akgül**[2]

Received: 11 November 2015 / Accepted: 18 April 2016 / Published online: 10 May 2016

Abstract This study presents a thermal analysis for a novel type of solar air heater. The thermal performance of a solar air collector having conical springs on the absorber plate is determined experimentally. A flat absorber plate (Type I) and the absorber plate with mounted conical springs (Type II) are designed and constructed, and their thermal performance is tested in the collectors. Experiments are performed for air mass flow rates of 0.06 and 0.07 kg/s. Thermal efficiency and collector outlet temperature are the main indicator for determining thermal performance. The efficiencies and energy distribution ratios are determined and compared for the collectors. The results of the experiments show that a substantial enhancement in the thermal efficiency is obtained with conical springs. Also, to this thermal efficiency increases with the rise of mass flow rate.

Keywords Solar air collector · Conical springs · Thermal efficiency · Obstacle · Absorber

1 Introduction

The demand for utilization of solar energy has been increasing in correlation to the rise in energy prices. Solar energy is used mainly in photovoltaic systems for generating electricity and in thermal collectors for air and liquid heating. Studies of thermal collectors are focused on the improvement of the air heating systems because they are relatively easy to manufacture and more used for in many applications from space heating to drying of agricultural products. Turkey has high solar energy potential due to it being well located in the northern hemisphere. The average annual sunshine duration is 2640 h (daily total 7.2 h), and the average annual solar radiation is 3.6 kWh/m^2 per day. For Manisa, September has 4.63 kWh/m^2 global radiation and 9.26 h sunshine duration as average values [1].

SACs are durable, lightweight, simple, low-cost devices without problems such as corrosion, wear, and tear. A conventional solar air collector consists of a well-insulated housing, an absorber plate placed inside the housing, and a transparent cover at the top. A fan may be used in the system depending on the airflow situations whether it is natural or forced flow. The most significant deficiency of the SACs is the low heat transfer coefficient between absorber plate and air; thus, the thermal efficiency is low. An extremely effective way of eliminating this problem is to use various surface geometries. Bekele et al. [2] investigated experimentally the thermohydraulic performance characteristics of SACs with delta-shaped obstacles mounted on the absorber plate. Delta-shaped obstacles mounted on the absorber plate are found superior to any other SAC previously studied. Hachemi [3] presented an experimental investigation of the thermal performance of offset rectangular plate fin absorber plates. He indicated that offset-type fins placed parallel to the fluid flow increase the thermal efficiency significantly. Another way of improving the thermal efficiency in SACs is to use of porous structures in the collector [4–6]. Aldabbagh et al. [7] investigated the thermal performances of single- and double-pass solar air heaters with steel wire mesh layers, which are used instead of a flat absorber plate. They found that a maximum efficiency of 83.65 % could be obtained by using a porous media instead of an absorber plate in the double-pass model proposed in their study. A significant increase

✉ Mesut Abuşka
mesut.abuska@cbu.edu.tr

1 Department of Machine, Akhisar Vocational School, Manisa Celal Bayar University, Manisa, Turkey

2 Department of Mechanical Engineering, Faculty of Engineering, Manisa Celal Bayar University, Manisa, Turkey

Fig. 1 Heat transfer model of the solar air collector

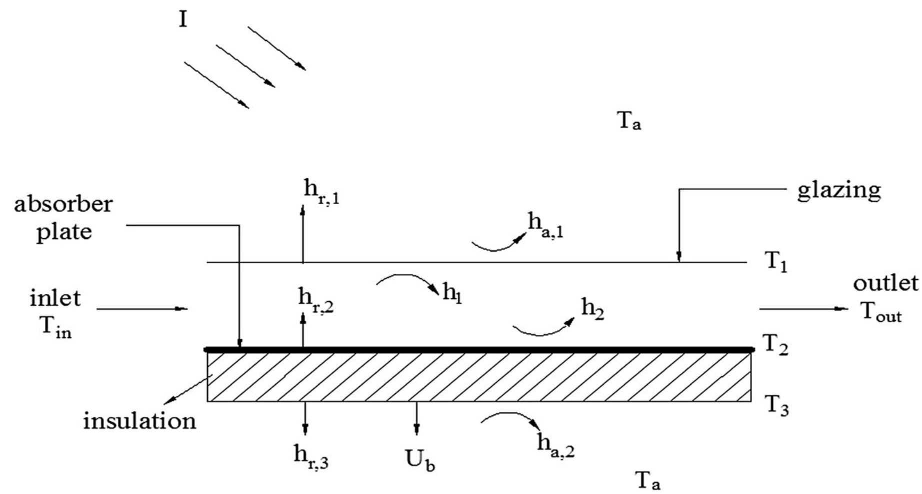

in the thermal efficiency may also be obtained with corrugated absorber plates in the collectors [8–11]. Esen [12] conducted an experimental energy and exergy analysis for a novel flat plate solar air heater with and without obstacles. He found that the usage of obstacles increased the thermal efficiency compared to the flat absorber plate. Benli [13] investigated the performance of five types of solar air absorbers and discussed the dependency of heat transfer coefficient and pressure drop according to the shape of absorber surface. Velmurugan and Kalaivanan [14] performed an analytical and experimental study of the energy and exergy performance of solar air heaters with various absorber plate geometries at different mass flow rates and solar intensities. Velmurugan and Kalaivanan [15] developed a mathematical model for predicting the thermal performance of double- and triple-pass solar air heater with fins. They found that the results of the analytical models were in good agreement with experimental findings of earlier researchers. Kabeel et al. [16] conducted an experimental investigation of flat and v-corrugated plate solar air heaters with built-in PCM as the thermal energy storage material. They state that thermal efficiency using PCM is 12 % higher than the corresponding ones without PCM.

In the literature, to the best knowledge of the authors of this article, there have been no studies conducted a thermal analysis of SACs with conical-shaped springs mounted on the absorber plate. Springs ensure proper airflow and reduce dead zones in the collector due to the structure. In this work, a novel SAC with conical springs mounted on the absorber plate is constructed and tested experimentally. The efficiencies and energy distribution ratios are determined and compared for the collectors. The organization of this paper is as follows: Sect. 2 describes the mathematical model used to calculate heat gains and losses depending on the environmental effects and system design. Section 3 gives the details of the experimental setup and technical specification of the system. In Sect. 4, the experimental results and calculations of energy distribution ratios and efficiency are given, and the effect of conical springs is discussed.

2 Mathematical Model

The heat transfer modeling of a solar air collector considered in this study is schematically shown in Fig. 1.

Here, I (W/m^2) is the solar radiation intensity, α_p and α_{g} are the absorptivity coefficients of the absorber plate and glazing, respectively. $h_{a,1}$ (W/m^{2}K) is the heat transfer coefficient between ambient air and glazing. $h_{a,2}$ (W/m^{2}K) is the heat transfer coefficient between ambient air and back surface of the collector. The transmittance of the glazing is τ_{g}. T_1, T_2, and T_3 (°C) are the temperatures of the glazing, absorber plate, and back surface of the collector, respectively. $h_{r,1}$ moreover, $h_{r,2}$ (W/m^{2}K) are the radiative heat transfer coefficients between the glazing and ambient, and glazing and absorber plate, respectively. U_b (W/m^{2}K) is the overall heat transfer coefficient between the back surface of the collector and the ambient. T_{f} (°C) is the working fluid temperature. h_1 (W/m^{2}K) is the heat transfer coefficient between the air and glazing, and h_2 (W/m^{2}K) is the heat transfer coefficient between the air and the absorber plate.

Assuming that the airflow is in steady state, the side surfaces of the collector are insulated perfectly, and the air temperature in the collector changes only in the airflow direction, and there is no air leakage from the collector; conservation equations of energy for each component can be written as follows:

For transparent cover (glazing):

$$I\alpha_{\mathrm{g}} = h_{a,1}(T_1 - T_a) + h_1(T_1 - T_{\mathrm{f}}) + h_{r,2}(T_1 - T_2) + h_{r,1}(T_1 - T_a) \quad (1)$$

For airflow:

$$\mathrm{mc}_p \frac{\mathrm{d}T_\mathrm{f}}{\mathrm{d}x} = h_1 \left(T_\mathrm{f} - T_1\right) + h_2 \left(T_2 - T_\mathrm{f}\right) \tag{2}$$

For absorber plate:

$$I\alpha_p \tau_\mathrm{g} = h_2 \left(T_2 - T_\mathrm{f}\right) + h_{r,2} \left(T_2 - T_1\right) + U_b \left(T_3 - T_a\right) \tag{3}$$

The thermal efficiency of the collector considering the energy distribution in the above equations is defined as follows:

$$\eta = \frac{Q_\mathrm{f}}{Q_s} \tag{4}$$

where Q_f (J) is the total amount of heat transferred to the air and is expressed as:

$$Q_\mathrm{f} = \dot{m} c_p \left(T_\mathrm{out} - T_\mathrm{in}\right) \tag{5}$$

here, $\dot{m}$ (kg/s), c_p (*J/kgK*), T_in, and T_out ($°C$) are the air mass flow rate, heat capacity, inlet air temperature, and outlet air temperature, respectively. The air mass flow rate is:

$$\dot{m} = \rho V A_o \tag{6}$$

here ρ (kg/m^3) is the air density, V (m/s) is the average outlet velocity of the air, and A_o (m^2) is the cross-sectional area of the collector outlet.

Q_s is the input solar energy determined by the following expression;

$$Q_\mathrm{s} = I A_a \tag{7}$$

where $A_a (m^2)$ is the solar collecting area of the absorber plate. The conservation of energy in the form of heat is expressed as:

$$Q_\mathrm{s} = Q_\mathrm{f} + Q_{\mathrm{g,loss}} + Q_{bc,\mathrm{loss}} + Q_{\mathrm{other,loss}} \tag{8}$$

where $Q_{\mathrm{g,loss}}$ is the heat loss from the collector glazing and it can be written as:

$$Q_{\mathrm{g,loss}} = (\mathrm{h}_{a,1} + h_{r,1}) A_\mathrm{g} (T_1 - T_a) \tag{9}$$

where $A_\mathrm{g} (m^2)$ is the glazing surface area.

$Q_{\mathrm{bc,loss}}$ (J) is the heat loss from the back surface of the collector and expressed as:

$$Q_{\mathrm{bc,loss}} = (\mathrm{h}_{a,2} + h_{r,3}) A_\mathrm{bc} (T_3 - T_a) \tag{10}$$

where A_bc(m^2) is the back surface of the collector.

The convective heat transfer coefficient due to the wind between the ambient air and the collector is proposed by McAdams [17] as:

$$\mathrm{h}_a = 5.7 + 3.8 V_a \tag{11}$$

where V_a (m/s) is the wind velocity. The radiative heat transfer coefficients between the glazing and environment and the back surface of the collector and environment can be given by Eqs. 12 and 13, respectively [18];

$$h_{r,1} = \frac{\sigma \left(T_1^2 + T_a^2\right)\left(T_1 + T_a\right)}{\left(1/\varepsilon_\mathrm{g} - 1\right)} \tag{12}$$

and

$$h_{r,3} = \frac{\sigma \left(T_3^2 + T_a^2\right)\left(T_3 + T_a\right)}{\left(1/\varepsilon_\mathrm{bc} - 1\right)} \tag{13}$$

where σ (W/m^2K^4) is the Stefan–Boltzmann constant and ε is the emissivity.

3 Experimental Setup and Equipment

The experimental setup was constructed at Celal Bayar University (38°55′N − 27°50′E), Manisa, Turkey. Experiments were performed in September 2014 at average ambient conditions with sunshine duration of 9.26 h and the global radiation of 4.63 kWh/m^2 in the region. The setup consisted of two main parts: SACs and measurement instruments. Each SAC in this study is made by the combination of a collector box, an absorber plate, insulation materials, a transparent cover, and air circulation fans. The detailed technical specifications of the collectors are collated in Table 1.

Table 1 Technical specifications of the collectors

Collector components	Technical specifications
Collector type	Single pass, active, flows over the absorber plate
Collector box	0.8 mm thickness and 1000 × 2000 × 200 mm in dimensions
Insulation	50-mm glass wool used for back and side insulations
Absorber plate	Made of aluminum with 900 × 1900 × 0.5 mm in dimensions
Glazing	3.2 mm, low iron tempered glass and solar energy transmittance of 90.7 %
Absorber coating	Emissivity, ε: 0.20–0.49, Absorptivity, α: 0.88–0.94
Fans	Power: 2 × 35 W, Volume flow rate: 225 m^3/h, Cross type

Fig. 2 The experimental setup

A photograph of the established experimental setup is shown in Fig. 2. Obstacles made of aluminum conical springs are placed to reduce the thermal resistance of the absorber plate. The conical springs are manufactured by extruding wire of 1000 mm long and 2 mm diameter on a universal lathe machine. Geometric properties of the springs are shown in Fig. 3. The placement of the 162 pieces of obstacles on the absorber plate and cross-sectional view of the collectors are shown in Figs. 4 and 5. The total heat transfer area of the conical springs attached to absorber plate is 2.7 m^2.

After the installation of the experimental setup, two collectors were operated under clear weather conditions from 9.00 a.m. to 17.00 p.m. with double replication. The experiments were carried out for two different mass flow rates of 0.06 and 0.07 kg/s. The measurement parameters include inlet and outlet air temperatures, glazing and back surface temperatures, absorber plate temperatures, outlet air velocity, and solar irradiance. All measurement points are shown in Fig. 6 in the experimental setup.

Measurement Points:

1. Solar irradiance value
2. Collector inlet temperature

3–4. Average outlet velocity of the air from the collector $((V_3 + V_4)/2)$

5–6. Average outlet temperature of the air from the collector $((\mathrm{T}_5 + T_6)/2)$

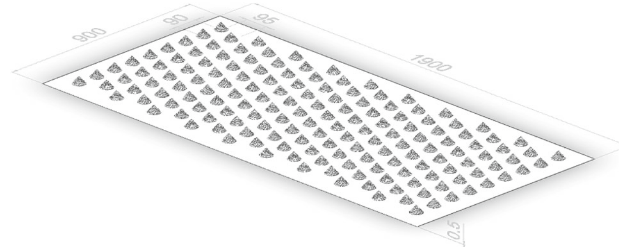

Fig. 4 Absorber plate with conical springs

7–8–9. Average surface temperature of the absorber plate $((\mathrm{T}_7 + T_8 + T_9)/3)$

10. Glazing surface temperature
11. Back surface temperature of the collector housing

12–13. Inlet and outlet pressures, respectively.

The flow rate is controlled by electric dimmer connected with fans. The velocity of the air is measured by hotwire-type anemometer with the precision of ± 0.2 m/s. Inlet and outlet air temperatures are measured by T-type thermocouples with the accuracy of $\pm 0.5\,^{\circ}$C. PT1000-type temperature probes with the accuracy of $\pm 0.15\,^{\circ}$C are used to measure surface temperatures of the glazing, absorber plate, and back surface of the collector housing. The total solar radiation incident on the glazing is measured by a pyranometer with an accuracy of $\pm 2\,\%$. Mass flow rate and thermal efficiency of the collectors are calculated based on the above experimental measurements. The total uncertainty belongs to mass flow rate, and thermal efficiency is 2.4 and 1.05 %, respectively.

4 Results and Discussion

The hourly variations of outlet air temperatures of Type I and Type II SACs at 0.06 and 0.07 kg/s mass flow rates are illustrated in Figs. 7 and 8, respectively. The total solar radiation value and ambient temperature variations during the experimental period are also shown in these figures. It is clear that the ambient temperature varies between 25 and 35°C during the experimental period. Global radiation sharply rises

Fig. 3 Geometric properties of the spring

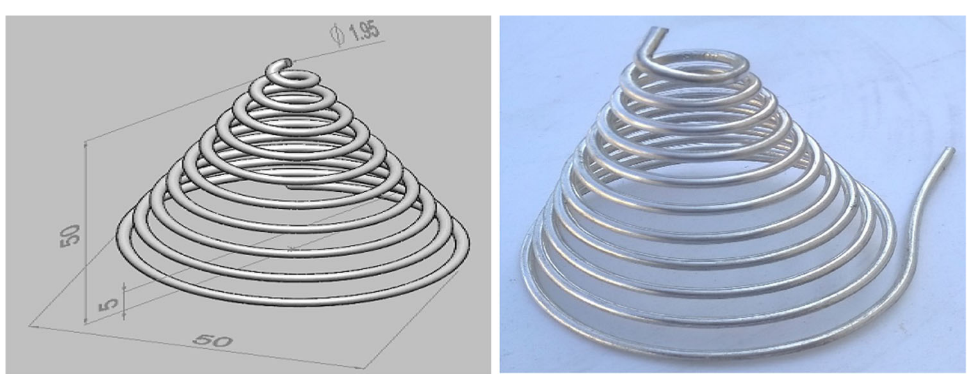

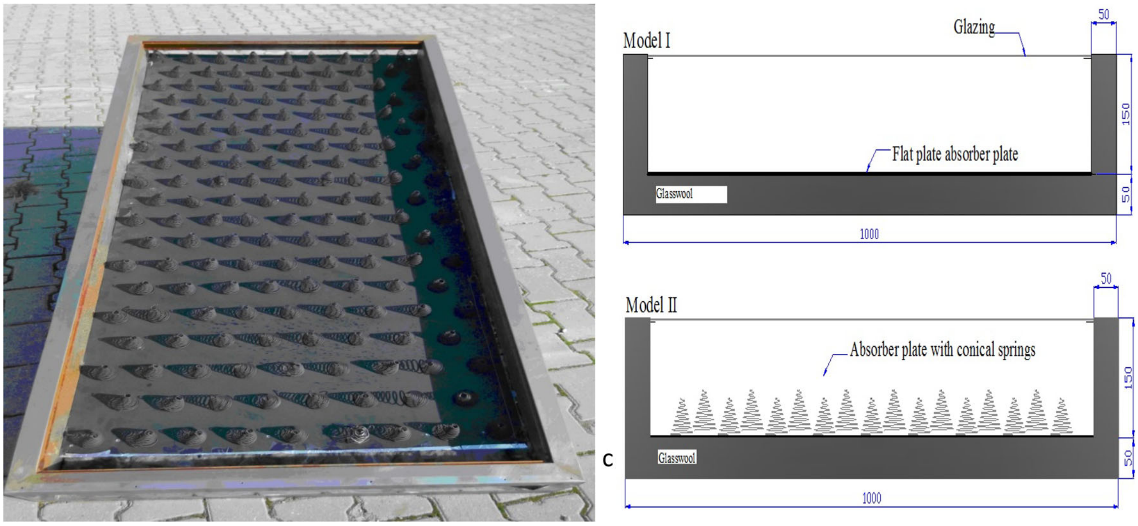

Fig. 5 Absorber plate in the collector box and cross-sectional view of the collectors

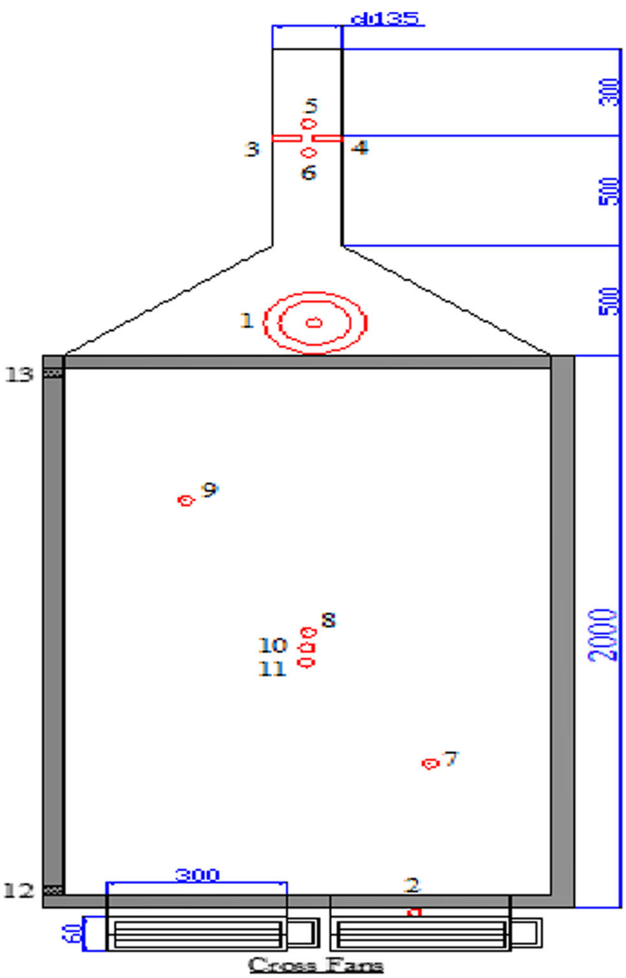

Fig. 6 Measurement points

from the morning to noon and reaches a maximum value at 13.00 p.m. In parallel with the change in the global radiation, collector outlet temperatures also show a similar trend. The outlet air temperature reaches a maximum value at noon for both collector types, as expected. It then starts to fall into decline in the afternoon. Results also show that the outlet temperature of the collector with conical springs mounted on the absorber plate (Type II) is higher than that of the flat plate collector (Type I). Moreover, a slight decrease in the outlet temperature is observed with increasing mass flow rate. This reason may be explained by residence time of air inside the collector.

The hourly variations of thermal efficiency of Type I and Type II solar air collectors at 0.06 and 0.07 kg/s mass flow rates are shown in Figs. 9 and 10, respectively. As seen in the figures, the thermal efficiency increases from the morning to noon and reaches a maximum value at 13.00 p.m. and then starts to decrease in the afternoon. The maximum thermal efficiency for 0.06 kg/s mass flow rate in Type I is 47.8 and 62.5 % in Type II. At a higher mass flow rate of 0.07 kg/s, thermal efficiencies for Type I and Type II are 50.4 and 65.9 %, respectively. Average efficiencies are given for both collector models at two different mass flow rate values in Fig. 11. It is clear that the average thermal efficiency of the collector with conical springs mounted on the absorber plate is higher than the flat one. As a result, the collector thermal performance is significantly improved by attaching conical springs on the absorber plate. Conical springs can be attributed to the increment of the heat transfer area and enhanced turbulent effects. Namely, the heat transfer area of the flat absorber plate is 1.71 m^2, whereas this value for Type II is 2.70 m^2. In addition to this, springs create turbulent effects in the collector and enhance heat transfer.

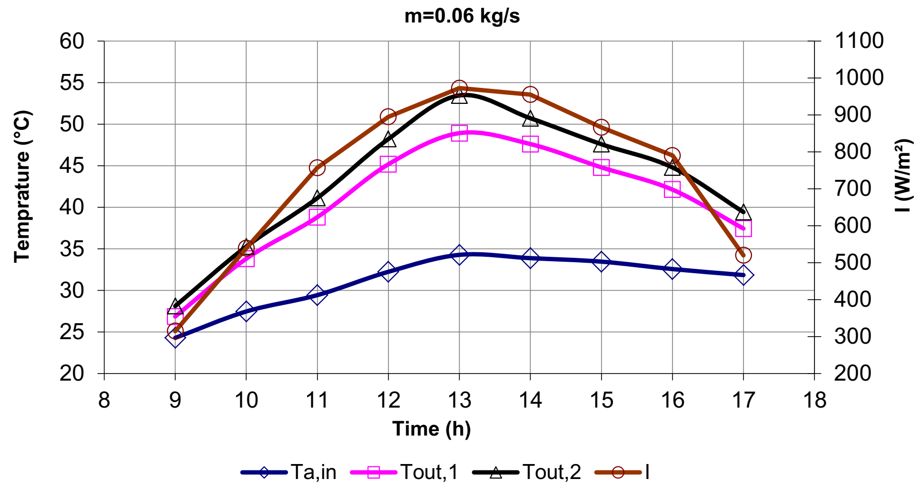

Fig. 7 Change of temperature with time, for $\dot{m} = 0.06\,\mathrm{kg/s}$

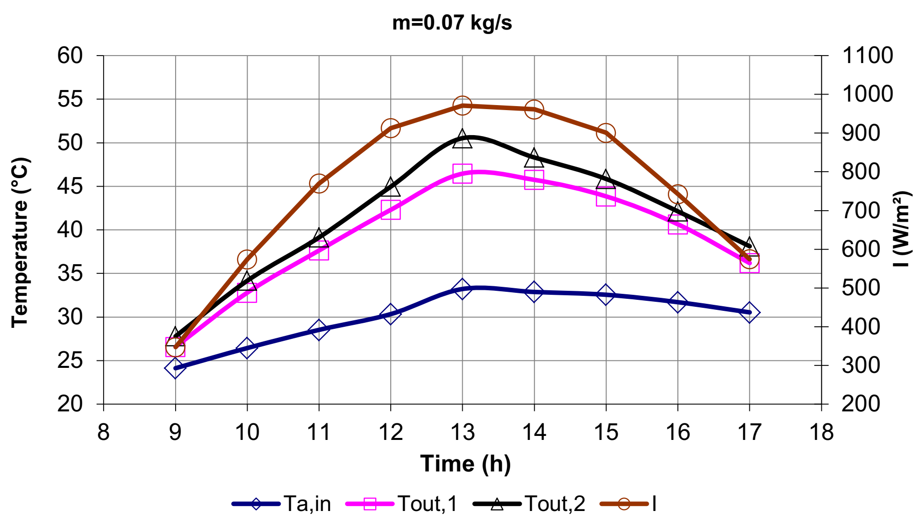

Fig. 8 Change of temperature with time, for $\dot{m} = 0.07\,\mathrm{kg/s}$

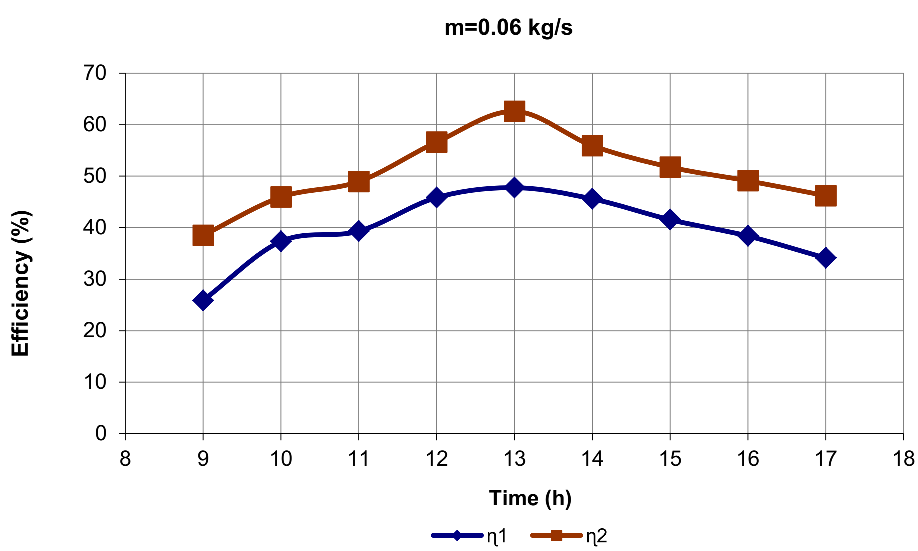

Fig. 9 Change of efficiency with time, for $\dot{m} = 0.06\,\mathrm{kg/s}$

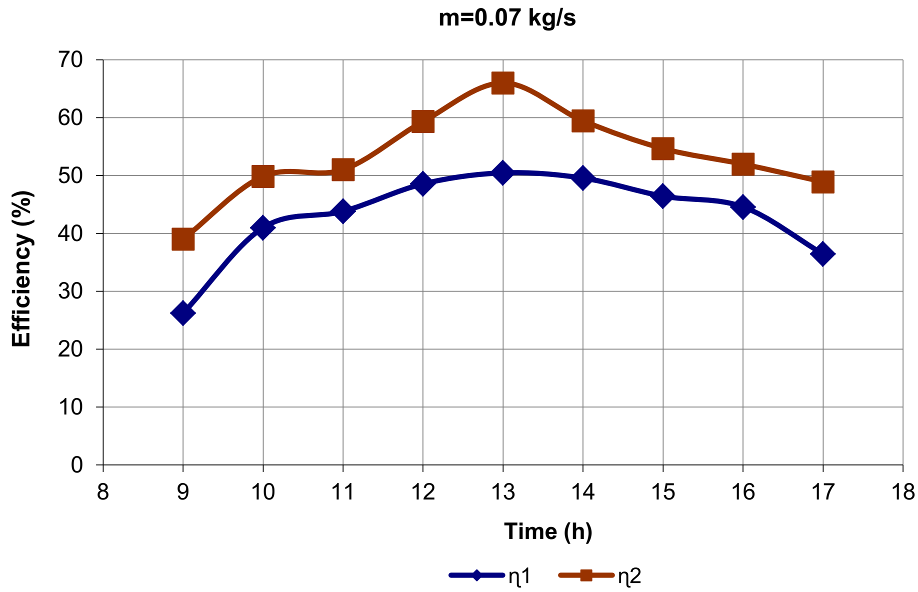

Fig. 10 Change of efficiency with time, for $\dot{m} = 0.07\,\mathrm{kg/s}$

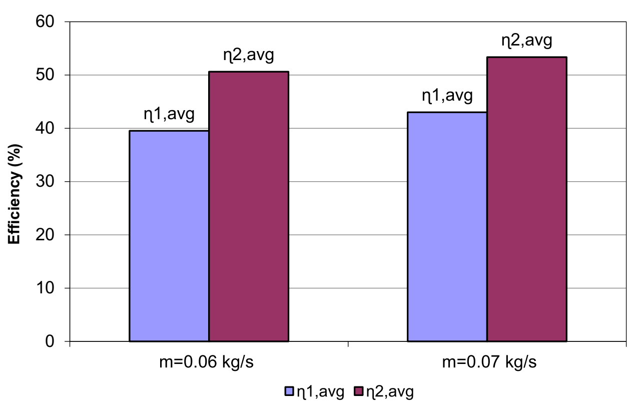

Fig. 11 Average thermal efficiency values for different mass flow rates

The average temperatures of the outlet air, exterior surfaces of the glazing cover and back plate are shown in Fig. 12. for both collector types at a mass flow rate of 0.06 kg/s. The outlet air temperature of Type II is 2.6°C higher compared with Type I. Besides, the lower exterior surface temperature at the glazing is observed for Type II. Backside temperatures of the collector housing are almost the same for both types.

The energy distribution ratios of the collectors are determined by the relations in the mathematical model and shown in Fig. 13. The sum of energy distribution ratios is constant and equals 100 %. The average values of global radiation, ambient temperature, and wind velocity are 735 W/m^2, 30.5°C, and 0.18 m/s, respectively. It is observed that the ratio of energy transferred to the air in the collector with conical springs

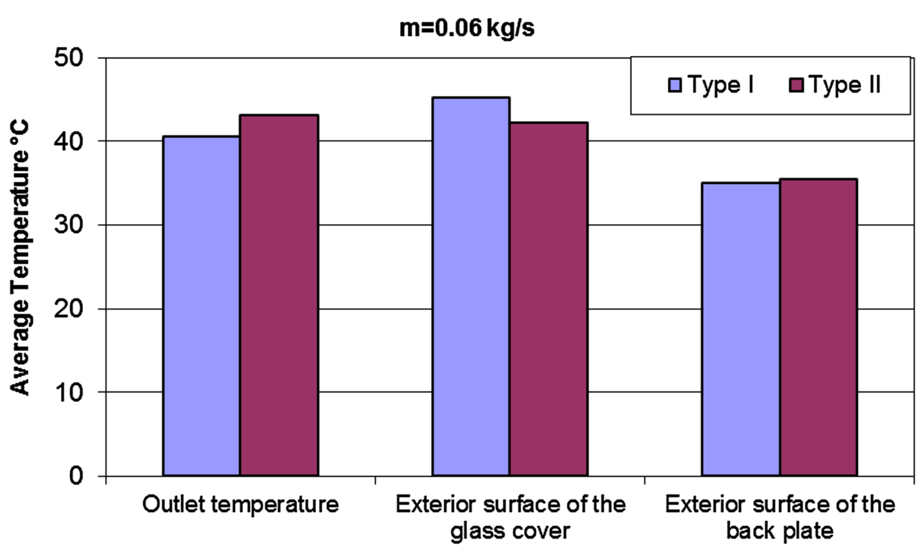

Fig. 12 Average surface temperatures

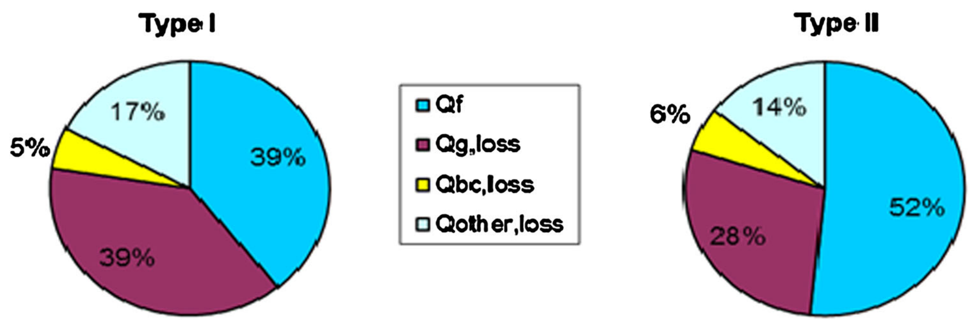

Fig. 13 Energy distribution ratios for $\dot{m} = 0.06$ kg/s

is 52 %. However, this value is 40 % for the flat plate collector. It can be explained by the increment of the heat transfer area and the enhanced turbulent effects. The largest energy loss in the both collectors is from the glazing surface. As a result of effective insulation, energy loss from the back plate is minimal for both collectors.

5 Conclusions

In this study, a novel SAC having conical springs attached to the absorber plate was designed, constructed, and compared experimentally with flat plate one. Thermal efficiency and collector outlet temperature are employed as the main indicator for determining thermal performance. The effectiveness of the solar air collectors depends significantly on the solar radiation, airflow rate, and surface geometry of the collectors. The maximum thermal efficiency is obtained as 50.4 and 65.9 % for both Type I and Type II, respectively, for 0.07 kg/s. The maximum average outlet temperature is obtained at 40.6 and 43.2°C for both Type I and Type II, respectively, for 0.06 kg/s. The ratio of energy transferred to the air in the collector is 52 and 40 % for both Type I and Type II, respectively, for 0.06 kg/s. As a result, significant heat transfer enhancement is observed for Type II comparing with Type I. The springs ensure a good air flow over the absorber plate, higher surface area, lower shadowing effect and reduce the dead zones in the collector. This novel design of the absorber plate with conical spring may be as energy efficient and economical alternative for known SACs.

Acknowledgments This work has been supported by the Scientific Research Project Coordination Unit of Celal Bayar University. The project number is 2013/024.

References

1. The Atlas of Solar Energy Potential: www.eiei.gov.tr (2007).
2. Bekele, A.; Mishra, M.; Dutta, S.: Performance characteristics of solar air heater with surface mounted obstacles. Energy Convers. Manag. **85**, 603–611 (2014)
3. Hachemi, A.: Experimental study of thermal performance of offset rectangular plate fin absorber-plates. Renew. Energy **17**(3), 371–384 (1999)
4. Omojaro, A.P.; Aldabbagh, L.B.Y.: Experimental performance of single and double pass solar air heater with fins and steel wire mesh as absorber. Appl. Energy **87**, 3759–3765 (2010)
5. Ramadan, M.R.I.; El-Sebaii, A.A.; Aboul-Enein, S.; El-Bialy, E.: Thermal performance of a packed bed double-pass solar air heater. Energy **32**, 1524–1535 (2007)
6. El-Sebaii, A.A.; Aboul-Enein, S.; Ramadan, M.R.I.; El-Bialy, E.: Year round performance of double pass solar air heater with packed bed. Energy Convers. Manag. **48**, 990–1003 (2007)
7. Aldabbagh, L.B.Y.; Egelioglu, F.; lkan, M.: Single and double pass solar air heaters with wire mesh as packing bed. Energy **35**, 3783–3787 (2010)
8. Mohammadi, K.; Sabzpooshani, M.: Comprehensive performance evaluation and parametric studies of single pass solar air heater with fins and baffles attached over the absorber plate. Energy **57**, 741–750 (2013)
9. Bayrak, F.; Öztop, H.F.; Hepbaşlı, A.: Energy and exergy analyses of porous baffles inserted solar air heaters for building applications. Energy Build. **57**, 338–345 (2013)
10. Abene, A.; Dubois, V.; Le Ray, M.; Ouagued, A.: Study of a solar air flat plate collector use of obstacles and application for the drying of grape. J. Food. Eng. **65**, 15–22 (2004)
11. Akpinar, E.K.; Kocyigit, F.: Energy and exergy analysis of a new flat-plate solar air heater having different obstacles on absorber plates. Appl. Energy **87**, 3438–3450 (2010)
12. Esen, H.: Experimental energy and exergy analysis of a double-flow solar air heater having different obstacles on absorber plates. Build. Environ. **43**, 1046–1054 (2008)
13. Benli, H.: Experimentally derived efficiency and exergy analysis of a new solar air heater having different surface shapes. Renew. Energy **50**, 58–67 (2013)
14. Velmurugan, P.; Kalaivanan, R.: Energy and exergy analysis of solar air heaters with varied geometries. Arab. J. Sci. Eng. **40**, 1173–1186 (2015)
15. Velmurugan, P.; Kalaivanan, R.: Thermal performance studies on multi-pass flat-plate solar air heater with longitudinal fins: An analytical approach. Arab. J. Sci. Eng. **40**, 1141–1150 (2015)
16. Kabeel, A.E.; Khalila, A.; Shalabyb, S.M.; Zayeda, M.E.: Experimental investigation of thermal performance of flat and v-corrugated plate solar air heaters with and without PCM as thermal energy storage. Energy Convers. Manag. **113**, 264–272 (2016)
17. McAdams, W.H.: Heat Transmission, 3rd edn. McGraw-Hill, New York (1954)
18. Naphon, P.; Kongtragool, B.: Theoretical study on heat transfer characteristics and performance of the flat-plate solar air heaters. Int. Commun. Heat Mass Transf. **30**, 1125–1136 (2003)